# Safe Link Mechanism based on Passive Compliance
# for Safe Human-Robot Collision

Jung-Jun Park, Byeong-Sang Kim, Jae-Bok Song, and Hong-Seok Kim

*Abstract*— A safe robot arm can be achieved by either passive or active compliance. The passive compliance systems composed of purely mechanical elements often provide faster and more reliable responses for dynamic collision than the active ones involving sensors and actuators. Since both positioning accuracy and collision safety are important, a robot arm should exhibit very low stiffness when subjected to the collision force greater than the one causing injury to humans, but maintain very high stiffness otherwise. To implement these requirements, a novel safe link mechanism (SLM), which consists of linear springs, a double-slider mechanism and shock absorbing modules, is proposed in this research. The main contribution of SLM lies in its variable stiffness capability implemented only by passive mechanical elements. Various experiments for static and dynamic collision show that the stiffness of SLM is kept very high for the external force less than the critical impact force, but it drops abruptly as the external force exceeds the critical force, thus guaranteeing the collision safety. Furthermore, the critical impact force can be set to any value depending on the applications.

## I. INTRODUCTION

For industrial robots, safe human-robot coexistence is not very important because the fast and precise manipulation is of main concern. However, service robots often interact directly with humans for various tasks. For this reason, safety has been one of the most important issues in service robotics. Therefore, several types of compliant joints and flexible links of a manipulator have been proposed for safety.

A safe robot arm can be achieved by either passive or active compliance. In the actively compliant arm, the collision is detected by various types of sensors and proper control action is performed to adjust its stiffness. The active compliance based approach suffers from the relatively low bandwidth because it involves sensing and actuation in a response to dynamics collision. This rather slow response can be improved slightly when non-contact sensors such as proximate sensors are employed. Furthermore, installation of the sensor and actuator in the robot arm often lead to high cost,

Jung-Jun Park and Byeong-Sang Kim are with the Dept. of Mechanical Eng., Korea University, Seoul, Korea (e-mail: hantiboy@korea.ac.kr, lovidia@korea.ac.kr).

Jae-Bok Song is a Professor of the Dept. of Mechanical Eng., Korea University, Seoul, Korea (Tel.: +82 2 3290 3363; fax: +82 2 3290 3757; e-mail: jbsong@korea.ac.kr)

Hong-Seok Kim is a Division Head of Control and Intelligence Research Team, Korea Institute of Industrial Technology, Ansan, Korea. (e-mail: hskim@kitech.re.kr)

an increase in system size and weight, possible sensor noise and actuator malfunction.

On the other hand, the robot arm based on passive compliance is usually composed of the mechanical components such as a spring and a damper to absorb the excessive collision force. Since this approach does not utilize any sensor or actuator, it can provide fast and reliable responses even for dynamic collision. Various safety mechanisms based on passive compliance have been suggested so far. The programmable passive impedance component using an antagonistic nonlinear spring and a binary damper was proposed to mimic the human muscles [1]. The mechanical impedance adjuster with a variable spring and an electromagnetic brake was developed [2]. The programmable passive compliance based shoulder mechanism using an elastic link was proposed [3]. A passive compliance joint with rotary springs and a MR damper was suggested for the safe arm of a service robot [4].

Most passive compliance based devices use linear springs. One drawback of using a linear spring is that positioning accuracy cannot be achieved because the spring always works even for small external forces which do not require any shock absorption and the elastic behavior of a spring often causes undesirable oscillations. To cope with this problem, some systems adopt the active compliance approach by incorporating extra sensors and actuators such as electric dampers or brakes, thereby significantly impairing the advantages of a passive system. In this research, therefore, a novel safety mechanism based on passive compliance is proposed to overcome the above problems.

Some tradeoffs are required between positioning accuracy and safety in the design of a manipulator because high stiffness is beneficial to the positioning accuracy whereas low stiffness is advantageous to the collision safety performance. It is desirable, therefore, that a manipulator should exhibit very low stiffness when subjected to the collision force greater than the one causing injury to humans, but maintain very high stiffness otherwise. Of course, this ideal feature can be achieved by the active compliance approach, but this approach often causes several shortcomings mentioned above.

In this research, this ideal feature is realized by a novel design of the safe link mechanism (SLM) which is based on the passive compliance. SLM is composed of the passive mechanical elements such as linear springs, a double-slider mechanism, and shock absorbing modules. The springs and shock absorbing modules are used to absorb the high collision force for safety, while the double-slider mechanism determines whether the external force can be regarded as the safe one or not and thus enables SLM to work only in case of

emergency. The main contribution of this proposed device lies in its variable stiffness capability implemented only by passive mechanical elements. Without a compromise between positioning accuracy and safety, both features can be achieved simultaneously with SLM.

The rest of the paper is organized as follows. The operating principle of SLM is discussed in detail in section II. Section III presents further explanation about its operation based on simulations. Various experimental results for both static and dynamic collision are provided in section IV. Finally, section V presents conclusions and future work.

## II. CONSTRUCTION OF SAFE LINK MECHANISM

The passive safety mechanism proposed in this research is composed of a spring, a double-slider mechanism and a shock-absorbing module-wire system. Section II.A presents the concept of the transmission angle of a double-slider mechanism and the characteristics of a double-slider combined with a spring. Section II.B deals with the construction of the shock-absorbing system.

### A. Double-slider mechanism

A spring has been widely used for a variety of safety mechanisms because it has an excellent shock absorbing property. Since the displacement of a linear spring is proportional to the external force, the robot arm exhibits deflection due to its own weight and/or payloads when a spring is installed at the manipulator joint. This characteristic is beneficial to a safe robot arm, but has an adverse effect on its positioning accuracy. To cope with this problem, it is desirable to develop a spring whose stiffness remains very high when the external force acting on the end-effector is within the range of the normal operation, but becomes very low when it exceeds a certain level of force due to collision with the object. It is obvious that no such springs with this ideal feature exist. In this research, the power transmission characteristics of the 4-bar linkage are exploited to achieve this nonlinear spring features.
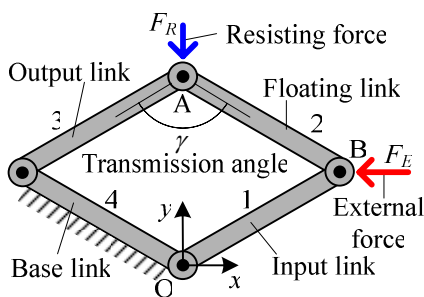


Fig. 1 4-bar linkage.

Consider a 4-bar linkage mechanism shown in Fig.1. When an external force $F_E$ is exerted on point B of the input link in the x-axis direction, an appropriate resisting force $F_R$ acting in the y-axis direction can prevent the movement of the output link. In the 4-bar linkage, the transmission angle is defined as the angle between the floating and the output link. The power transmission efficiency from the input to output varies

depending on this transmission angle. If the transmission angle $\gamma$ is less than 45° or greater than 135°, a large force is required at the input link to move the output link. That is, only small $F_R$ is sufficient to prevent the output link from moving for a given $F_E$ in this case. However, as the transmission angle approaches 90°, the power transmission efficiency improves, thus leading to easy movement of the output link of a 4-bar linkage [5].
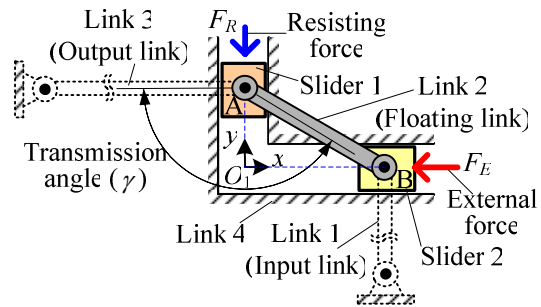


Fig. 2 Double-slider mechanism.

The 4-bar linkage can be converted into a double-slider mechanism shown in Fig. 2. If the output link (link 3) is assumed to be infinite and located in the x-axis direction, then revolute joint A between link 2 and link 3 can move in a rectilinear fashion only in the y-axis direction. Likewise, if the input link (link 1) is assumed to be infinite and located in the y-axis direction, then joint B can move only in the x-axis direction. In this case, the 4-bar linkage can be regarded as a double-slider mechanism. Note that the transmission angle of a double-slider mechanism can be also defined as the angle between the floating link (link 2) and the output link. The force balance of the forces acting on sliders 1 and 2 can be given by

$$F_R = -F_E \tan \gamma \qquad (1)$$

Note that the value of $\tan \gamma$ is always negative because $\gamma$ is in the range of $90^o$ to $180^o$ in Fig. 2, thus requiring the minus sign in (1). In (1), for the same external force, the resisting force changes as a function of $\gamma$.
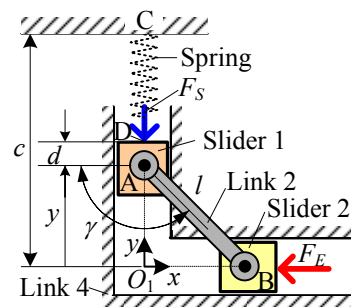


Fig. 3 Double-slider mechanism combined with spring.

If the pre-compressed spring is installed between points C and D in Fig. 3, the spring force $F_S$ can offer the resisting force $F_R$, which resists the movement of slider 1 caused by the

external force $F_E$. When the external force is balanced against the spring force, the external force can be described in term of the transmission angle and the other geometric parameters as follows:

$$F_E = -k(s_o - c + d + l\sin\gamma)\cot\gamma \qquad (2)$$

where $k$ is the spring constant, $s_o$ the initial length of the spring, $l$ the length of link 2, and $y$ the displacement of slider 1. Although $y$ does not explicitly appear in (2), it is directly related to $\gamma$ by the relation of $y = l\cos(\gamma - 90^o)$. For example, when $k$ = 10kN/m, $l$ = 19mm, $s_0$ = 34mm, $c$ = 36mm and $d$ = 6.5mm, the external force for the static force balance can be plotted as a function of $\gamma$ in Fig. 4. Note that it is needless to specify the spring force for the static balance because it is automatically determined for given $\gamma$. As shown in the figure, the external force diverges rapidly to the positive infinity as $\gamma$ approaches 180°, so even a very small spring force can make this mechanism statically balanced against a very large external force. In this research, the transmission angle in the range of 160° to 170° is mainly used by considering the mechanical strength of the mechanism.
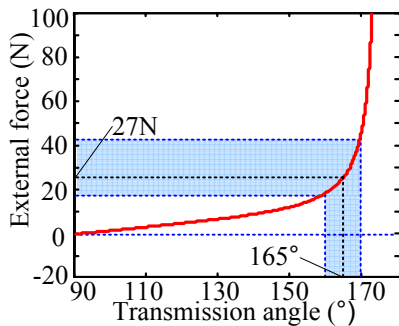

Fig. 4 External force as a function of transmission angle.

In this proposed mechanism, the external force required for balance with the spring force is defined as the *critical impact force*. For given $\gamma$, a static balance is maintained when the external force equals the critical impact force, as shown in Fig. 4, but the spring is rapidly compressed once the external force greater than this critical value acts on this mechanism. The detailed explanation about this phenomenon is given below.
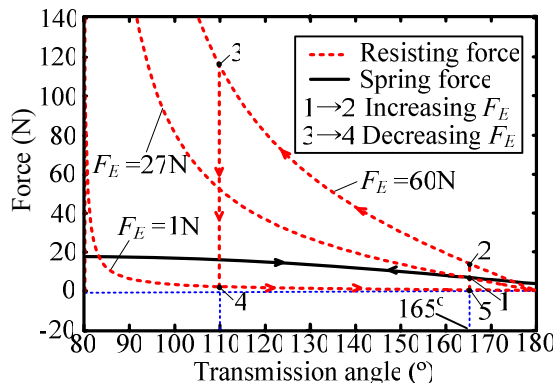

Fig. 5 Plots of resisting force and spring force versus transmission angle at high and low critical impact forces.

Figure 5 shows the resisting force curves for the three given external forces ($F_E$ = 1, 27, 60N) as a function of the transmission angle $\gamma$, which is computed by (1). The spring force as a function of $\gamma$ is also plotted in Fig. 5. Note that the variation of the spring force is much smaller than that of the resisting force throughout the wide range of $\gamma$. Since the spring force provides the resisting force, when these two forces are equal, the static balance of the mechanism shown in Fig. 3 can be achieved.

Suppose the critical impact force is set to 27N. Then the transmission angle $\gamma$ for the static equilibrium becomes 165° from (2) with $F_E$ = 27N. This corresponds to equilibrium point 1, which is the intersection of the resisting force curve of $F_E$ = 27N and the spring force curve. Now suppose the external force abruptly increases to 60N which is larger than the critical impact force (1→2), then $\gamma$ reduces as slider 1 moves up in Fig. 3. As $\gamma$ decreases, the resisting force rapidly increases (2→3) and the spring force also slightly increases, as shown in Fig. 5. Since the resisting force required for the static equilibrium becomes much larger than the spring force, the static equilibrium cannot be maintained, thus causing slider 1 to move up rapidly. When the external force is reduced to 1N which is less than the critical impact force (3→4), the spring force becomes larger than the resisting force required and $\gamma$ increases because slider 1 is pushed down (4→5) by the spring force.

*B. Shock-absorbing system*

A rigid-plastic material such as a crash panel and an automobile bumper does not deform under normal operation, but must deform plastically and absorb the shock in case of an accident involving a large impact [6]. It deforms when subjected to more than the critical stress and absorbs the shock during this plastic deformation. This feature is well suited for the safety mechanism, but it cannot be restored to its original shape after deformation. To overcome this disadvantage, a shock-absorbing wire–module device is proposed below.
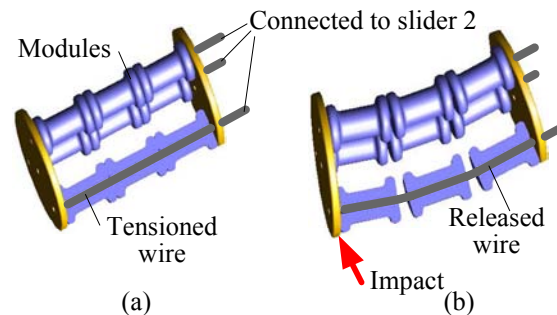

Fig. 6 Shock-absorbing system composed of modules and wire; (a) before collision, and (b) after collision.

As shown in Fig. 6(a), the small cylindrical modules are connected in series by a wire. Under normal operation, these modules remain tightly connected together by the tensioned

wire. One end of the wire is attached to the left of slider 2 in Fig. 3. Suppose a large impact greater than the critical impact force is applied to one end of the system, as shown in Fig. 6(b). This large external force causes slider 2 to move slightly to the left by the wire tension. This then breaks the static balance and moves slider 2 abruptly to the left, thus making the wire loose. This loose wire makes the modules disintegrated, which absorbs the impact force effectively, as shown in Fig. 6(b). This phenomenon will be explained in more detail in the next section.

## III.   SAFE LINK MECHANISM MODEL

### A.  Prototype modeling

The mechanisms introduced conceptually in the previous section are now integrated into the Safe Link Mechanism (SLM), which suggests a new concept of safe robot arm. SLM consists of a double-slider mechanism, a linear spring and a module-wire system, as shown in Fig. 7. As shown in Fig. 7, the moving plate (link 4 in Fig. 3) can slide relative to the fixed plate (slider 2 in Fig. 3) along the prismatic joint (P-joint) composed of a linear busing guide. Note that a combination of fixed link 4 and an assembly of slide 1 and the spring, which could not move in the *x*-axis direction in Fig. 3, are now allowed to move, whereas moving slider 2 in Fig. 3 now functions as a fixed plate in Fig. 7.
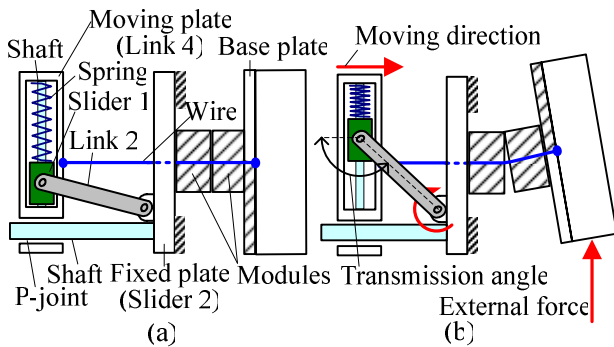


Fig. 7 Operation of SLM; (a) before collision, and (b) after collision.

If the external force exceeding the critical impact force is applied to a base plate shown in Fig. 7(b), then the moving plate is pulled toward the fixed plate by a wire connected to the base plate. Then, slider 1 linked to link 2 is forced to move up the guide shaft to compress the spring. This movement of slider 1 reduces the transmission angle, so maintaining the static balance requires a greater resisting force for the same external force. However, the increased spring force due to its compression is not large enough to sustain the balance. This unbalanced state causes slider 1 to rapidly slide up, thus bringing the moving plate further toward the fixed plate. As a result, the wire becomes loose and the modules are disintegrated, thus absorbing the external force, as explained before. However, if the external force is less than the critical impact force, the base plate does not move at all, and the

modules remain tightly connected together, thus providing high stiffness to SLM.

### B.  Simulations of Prototype

Various simulations have been conducted to evaluate the performance of the proposed SLM. The components of the mechanism were modeled by Solidworks and its dynamics was analyzed by Visual Nastran 4D. For simplicity of simulation, only the double-slider mechanism of SLM was modeled by assuming that the external force directly acted on the center of the moving plate. Slider 1 moving on the guide shaft was modeled as a spring-damper system. The damper was modeled to represent the friction between the slider and the shaft, although a damper was not used for the real system.
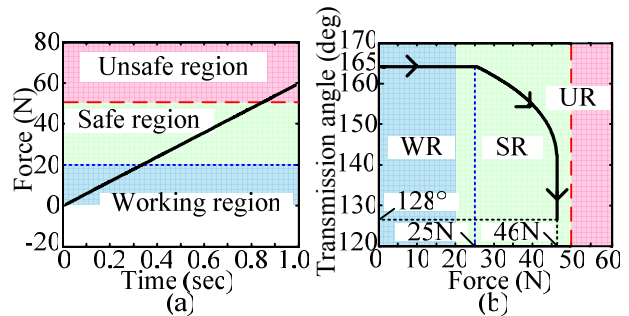


Fig. 8 Simulation results for static collision for initial transmission angle of 165º; relation between (a) external force and time, and (b) transmission angle and external force.

Figure 8 shows the simulation results for static collision. As the external force acting on the moving plate increases linearly up to 60N during 1sec, the change in transmission angle was observed in Fig. 8(b). In this simulation, the damping coefficient *c* was set to 2kg/s, the spring constant to *k* 10kN/m, the initial length of the spring $s_o$ to 34mm and the initial transmission angle to 165°. As shown in Fig. 8(b), the transmission angle does not change for the external force less than the critical impact force (in this simulation, 25N). However, once the external force exceeds the critical impact force, the transmission angle is on the sharp decrease. In summary, SLM stiffness remains very high while the external force is below 25N like a rigid link. In the range of 25 to 46N, the transmission angle decreases, thereby lowering the stiffness. As the external force approaches 46N, the stiffness abruptly diminishes, thus causing SLM to behave as a flexible link.

## IV.   EXPERIMENTS FOR SAFE LINK MECHANISM

### A.  Prototype of SLM

The prototype of SLM shown in Fig. 9 was constructed to conduct various experiments related to the performance of SLM. Most components are made of duralumin which can endure the shock exerted on SLM. The moving plate can translate relative to the fixed plate by means of the linear bushing guides which are able to reduce friction.
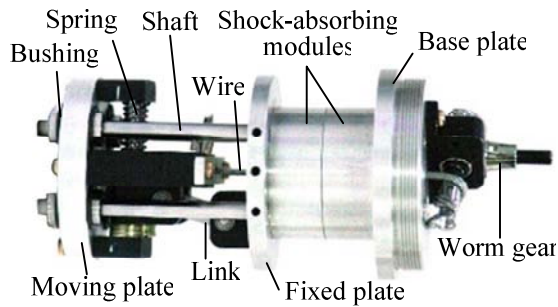
Fig. 9 Prototype of SLM.

As shown in Fig. 10(a), the initial transmission angle can be adjusted physically by inserting some thin plates between the slider and the shaft end block. The contact surface of one module has a convex hemisphere, while that of another module has a concave shape, so that the twist between the modules could be prevented. The wire is made of stainless steel which can endure to the shock. The wire tension can be adjusted by means of the worm and worm gear.
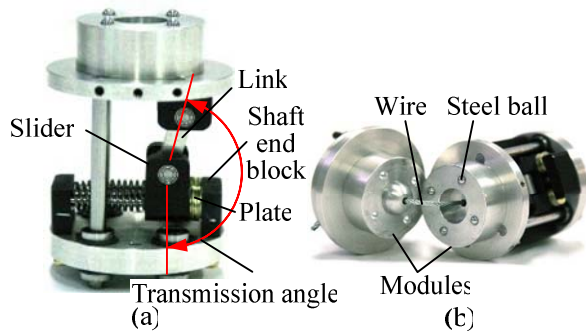


Fig. 10 Components of safety mechanism; (a) plates inserted for adjustment of transmission angle, and (b) appearance of modules.

### B. Safety criterion

The safety criterion can be divided into static and dynamic collision. The static collision means that the collision speed between the robot arm and a human is very low (e.g., below 0.6m/s). The human pain tolerance for static collision can be expressed by

$$F \leq F_{\text{limit}} \tag{8}$$

where $F_{limit}$ is the injury criterion value which has been suggested as 50N by several experimental researches [7].

In case of dynamic collision, both the collision force and the collision speed are important. To represent the human safety associated with the dynamic collision of SLM, the head injury criterion (HIC) used to quantitatively measure the head injury risk in car crash situations is adopted in this research [8].

$$HIC = T \left( \frac{1}{T} \int_0^T a(t)dt \right)^{2.5} \tag{9}$$

where $T$ is the final time of impact and $a(t)$ is the acceleration in the unit of the gravitational acceleration $g$. An HIC value of 1,000 or greater is typically associated with extremely severe head injury, and a value of 100 can be considered suitable to normal operation of a machine physically interacting with humans.

### C. Experimental results

Figure 11 shows an experimental setup in which SLM is installed at the 1-DOF robot arm. A force/torque sensor is installed at the end-effector of the arm to measure the collision force. The displacement of SLM is measured by an encoder attached to SLM.
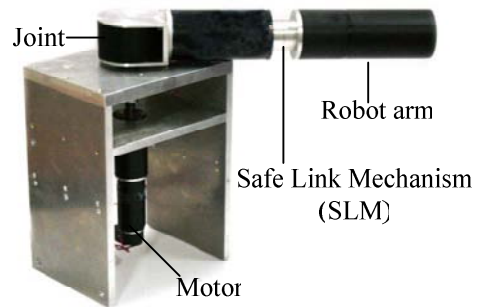


Fig. 11 Experimental setup for robot arm with SLM.

In the experiment for static collision, the spring constant was 10kN, its initial length was 34mm, and the transmission angle was 165°. The end-effector of the robot arm was initially placed to barely touch a fixed wall, and its joint torque provided by the motor was increased slowly. The static collision force between the robot and the wall was measured by a force/torque sensor. Experiments were conducted for the robotic arms with and without SLM.
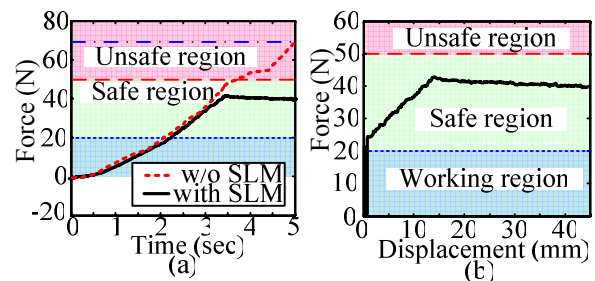


Fig. 12 Experimental results for static collision of robot arm; (a) collision force vs. time with and without SLM, (b) collision force vs. displacement of end-effector with SLM.

The robot arm without SLM delivered a contact force up to 70N to the wall, whereas the maximum contact force by the robot arm with SLM was only 40N, as shown in Fig. 12(a). In other words, the contact force above the pain tolerance does not occur because the excessive force is absorbed by SLM. In Fig. 12(b), virtually no displacement of the robot arm occurs when the contact force is below the critical impact force of 27N. Therefore, the robot arm with SLM can accurately handle the payload up to approximately 2.7kg as if it were a

very stiff link. As the contact force rises above the critical impact force, SLM stiffness quickly diminishes, thus maintaining the robot arm in the safe region. In summary, SLM provides the high positioning accuracy of the robot arm in the working region, while the safe human-robot contact can be guaranteed by absorbing the contact force above 50N in the unsafe region.

Next, some experiments for dynamic collision were conducted for the robot arm equipped with SLM. The experimental conditions including the spring constant, the initial length of the spring, and the initial transmission angle were set to the same as the static collision experiments. For dynamic collision, a plastic ball of 1.5kg moving at a velocity of 3m/s was forced to collide with the end-effector of the robot arm. The acceleration of the ball was measured by the accelerometer mounted at the ball.
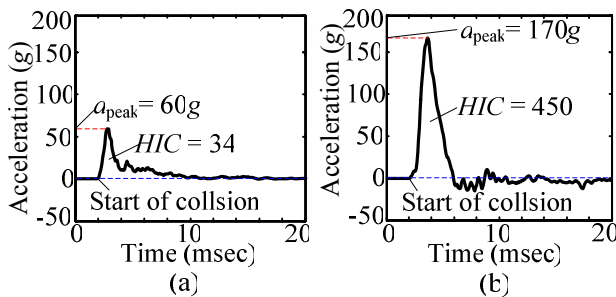


Fig. 13 Experimental results for dynamic collision of robot arm; acceleration vs. time (a) with SLM, (b) without SLM.

The experimental results are shown in Fig. 13. At the instant the ball contacts the end-effector, the acceleration of the ball reached a peak value of $60g$, but immediately after collision, the collision force delivered to the ball dropped rapidly because of the operation of SLM. The dynamic collision safety of the robot arm with SLM can be verified in terms of HIC defined by (9). The HIC value was computed as 34, which is far less than 100. Therefore, the safe human-robot contact can be achieved even for this harsh dynamic collision.

Figure 13(b) shows the experimental results for the dynamic collision of the robot arm without SLM. The peak value of the acceleration is almost triple that of the robot arm with SLM, and the HIC value reached as high as 450, which is high enough to cause injury to a human. Therefore, the robot arm with SLM provides much higher safety for human-robot contact than that without SLM.

## V. CONCLUSIONS

In this research, the safe link mechanism (SLM) has been proposed. SLM maintains very high stiffness up to the pre-determined critical impact force, but provides very low stiffness above this critical value, thus absorbing the impact acting on the robot arm. From the analysis and experiments, the following conclusions are drawn:

1) SLM has very high stiffness like a rigid arm when the external force acting on it is less than the critical impact

force. Therefore, high positioning accuracy of the robot arm can be achieved in normal operation.

2) When the external force exceeds the critical impact force, the stiffness of SLM abruptly drops. As a result, the robot arm acts as a flexible arm with high compliance. Therefore, human-robot collision safety can be attained even for dynamic collision with high speed.

3) The critical impact force of SLM can be set accurately by adjusting the initial transmission angle of the double-slider mechanism, the spring constant and the initial spring length.

4) The proposed SLM is based on passive compliance, so it shows a fast response and high reliability compared with the active compliance based mechanisms having sensors and actuators.

5) If SLMs are applied to more than two links of a robot arm, it can absorb the omni-directional impact force and the shock-absorbing range can increase. Therefore, some limitations of SLM can be overcome in various collision conditions.

Currently, the simpler and lightweight safe link mechanism which does not use the wire is under development. Furthermore, the research on the safe joint mechanism possessing the similar characteristics is under way.

## REFERENCES

[1] K. F. Laurin-Kovitz and J. E. Colgate, "Design of components for prog rammable passive impedance," *Proc. of the IEEE International Conf erence on Robotics and Automation*, pp.1476-1481, 1991.

[2] T. Morita and S. Sugano, "Development of one-D.O.F. robot arm equi pped with mechanical impedance adjuster," *Proc. of the IEEE/RSJ Int ernational Conference on Intelligent Robots and System*, pp. 407-41 2, 1995.

[3] M. Okada, Y. Nakamura and S. Ban, "Design of programmable passiv e compliance shoulder mechanism," *Proc. of the IEEE International Conference on Robotics and Automation*, pp.348-353, 2001.

[4] S. Kang and M. Kim, "Safe Arm Design for Service Robot," *Proc. of t he International Conference on Control, Automation and System*, pp. 88-95, 2002.

[5] C. E. Wilson and J. P. Sadler, *Kinematics and Dynamics of Machinery*, 2nd Edition, HaperCollins, 1993.

[6] S. H. Crandall and N. C. Dahl, *An Introduction to the Mechanics of So lids*, 2nd Edition, McGraw-Hill, 1978.

[7] Y. Yamada, Y. Hirasawa, S.Y. Huang and Y. Umetani, "Fail-safe hum an/robot contact in the safety space," *IEEE International Workshop on Robot and Human Communication*, pp. 59-64, 1996.

[8] J. Versace, "A review of the severity index," *Proc. of the 15th Stapp C ar Crash Conference,* pp.771–796, 1971.